

## ORIGINAL ARTICLE

# Obesity in C57BL/6J mice is characterized by adipose tissue hypoxia and cytotoxic T-cell infiltration

ME Rausch<sup>1</sup>, S Weisberg<sup>2</sup>, P Vardhana<sup>1</sup> and DV Tortoriello<sup>1,2</sup>

<sup>1</sup>Division of Reproductive Endocrinology, Department of Obstetrics and Gynecology, Columbia University, New York, NY, USA and <sup>2</sup>Division of Molecular Genetics, Department of Pediatrics, Columbia University, New York, NY, USA

**Background:** Obesity is currently viewed as a state of chronic low-grade inflammation in which there is a pro-inflammatory alteration in the serum adipocytokine profile as well as an infiltration of white adipose tissue by activated macrophages. The etiology of this inflammation, however, is poorly understood.

**Methods:** Hypothesizing that local hypoxia within expanding white adipose tissue depots may contribute to obesity-related inflammation, we compared body composition, serum inflammatory marker concentrations and the expression of several hypoxia-regulated genes in white adipose tissue derived from lean, dietary-induced obese (DIO) and *ob/ob* male C57BL/6J mice. We also examined white adipose tissue for the presence of hypoxia using both a pimonidazole-based antibody system and a fiberoptic sensor for real-time  $pO_2$  quantification *in vivo*. Finally, using cell-specific leukocyte antibodies, we performed immunohistochemistry and flow cytometric analyses to further characterize the cellular nature of adipose inflammation.

**Results:** We determined that obesity in male C57BL/6J mice is associated with increased expression of HIF (hypoxia-inducible factor) isoforms and GLUT-1, and that white adipose tissue hypoxia was present in the obese mice. Immunohistochemistry revealed hypoxic areas to colocalize predominantly with F4/80+ macrophages. Interestingly, CD3+ T cells were present in large numbers within the adipose of both DIO and *ob/ob* obese mice, and flow cytometry revealed their adipose to possess significantly more CD8+ T cells than their lean cohort.

**Conclusions:** White adipose hypoxia and cytotoxic T-cell invasion are features of obesity in C57BL/6J mice and are potential contributors to their local and generalized inflammatory state.

*International Journal of Obesity* (2008) 32, 451–463; doi:10.1038/sj.ijo.0803744; published online 25 September 2007

**Keywords:** adipose; hypoxia; inflammation; T cells

### Introduction

Obesity is a world-wide epidemic.<sup>1,2</sup> Data from the National Health and Nutrition Examination Surveys show that approximately 62 and 34% of the adult population in the United States are overweight or obese, respectively, and these figures have increased by approximately 10% between National Health and Nutrition Examination Surveys III (1988–1994) and National Health and Nutrition Examination Surveys 1999–2002.<sup>3–5</sup> Unfortunately, the situation is likely to worsen significantly given the greatest increase in the prevalence of obesity appears to be in young children.<sup>6</sup>

Research utilizing mice that were made obese either from leptin gene deletion (*ob/ob*) or from high-fat diet (dietary-

induced obese or DIO) has recently led to the identification of obesity as a state of chronic low-grade systemic inflammation whose epicenter appears to reside within white adipose tissue.<sup>7</sup> This inflammation has been postulated to underlie the development of obesity's associated medical complications, which include type 2 diabetes, atherosclerosis and dyslipidemia.<sup>8–11</sup> Characteristics of obesity-associated inflammation include increased serum concentrations of pro-inflammatory molecules produced by adipose tissue, liver and skeletal muscle<sup>7,12–17</sup> such as acute-phase reactants, thrombogenic factors, cytokines, and chemokines<sup>10,18</sup> and the activation of the JNK and NF- $\kappa$ B pathways, which are integral to the inflammatory process.<sup>16,19–21</sup> Although the inciting event that triggers the inflammatory cascade in adipose tissue remains to be elucidated, macrophages, which accumulate within the adipose tissue of the obese and can produce several pro-inflammatory molecules,<sup>7,22,23</sup> are believed to significantly modulate this process.

Given the prodigious ability of adipose tissue to enlarge rapidly during the acquisition of obesity, we hypothesized

Correspondence: Dr DV Tortoriello, Department of Obstetrics and Gynecology, Russ Berrie Medical Science Pavilion, Columbia University Medical Center, The New York Presbyterian Hospital, 1150 St Nicholas Avenue, Room 620, New York, NY 10032, USA.  
E-mail: dt2016@columbia.edu

Received 6 March 2007; revised 10 August 2007; accepted 19 August 2007; published online 25 September 2007

that intermittent local hypoxia may occur within white adipose tissue as it expands ahead of its vascular support, thereby initiating or, at the very least, augmenting the inflammatory reaction. We tested our hypothesis by quantifying the expression of hypoxia-upregulated genes, namely hypoxia-inducible factor (HIF), a key regulator of angiogenesis when metabolic demand exceeds the oxygen supply,<sup>24</sup> and GLUT-1, the main glucose transporter of macrophages, in the perigonadal adipose tissue of lean, DIO and *ob/ob* C57BL/6J mice. In addition, we examined their adipose tissue for hypoxia at the cellular level using a pimonidazole-based antibody system and also *in vivo* using an oxygen-sensing fiberoptic probe. Furthermore, in an effort to characterize the relationship between adipose tissue hypoxia and the inflammatory reaction associated with it, we performed immunohistochemistry and flow cytometric analyses upon adipose tissue from lean and obese mice using several leukocyte-specific antibodies.

We determined that the relative adipose tissue expression of HIF-1 $\alpha$ , HIF-2 $\alpha$  and GLUT-1 as well as the presence of pimonidazole-detected intracellular hypoxia is increased in DIO and *ob/ob* male C57BL/6J mice compared to lean controls. Real-time  $pO_2$  assessment using a tissue oxygen sensor showed that both DIO and *ob/ob* obese mice had significantly lower adipose tissue  $pO_2$  levels than lean controls. Pimonidazole-detected hypoxic areas were noted to colocalize predominantly with F4/80+ macrophages. We also discovered that, in addition to macrophage accumulation, the inflammatory reaction within the adipose tissue of C57BL/6J male mice made obese from either high-fat diet (DIO) or leptin gene deletion (*ob/ob*) is also characterized by a striking influx of CD8+ T cells.

## Materials and methods

### Experimental animals

We repeatedly utilized three experimental mice groups in this study. The first group was the 'lean' group, which consisted of wild-type male C57BL/6J mice fed a standardized low-fat diet (4% by weight, D12450B-I, Research Diets, New Brunswick, NJ, USA) from age 3 weeks onward; a 'DIO' group, which consisted of wild-type male C57BL/6J mice fed a standardized high-fat diet (35% fat by weight, D12451-i, Research Diets) from age 3 weeks onward; and the '*ob/ob*' group, which consisted of male C57BL/6J mice homozygous for the leptin knock-out *ob* mutation, which were fed the same low-fat diet as the 'lean' group.

Mice were obtained from the Jackson Laboratory (Bar Harbor, ME, USA) at approximately 3–5 weeks of age. They were housed five in a cage and maintained on a 14:10 light–dark cycle with *ad libitum* access to food and water. All mice remained on their assigned diet until killed by CO<sub>2</sub> asphyxiation at the age of approximately 24–28 weeks. All protocols were conducted in accord with the National Institutes of Health guide for the care and use of laboratory

animals and were approved by the Columbia University Animal Care and Use Committee.

### Body composition analysis

The body percentages of fat and lean tissue were calculated from exsanguinated carcasses by dual energy X-ray absorptiometry (DEXA) using a Lunar PIXImus2 machine (GE Medical Systems, Waukesha, WI, USA). DEXA uses two different low-dose X-rays to read bone and soft tissue mass with a high degree of precision.

### Real-time PCR quantification of white adipose tissue HIF expression

Immediately after killing, a portion of perigonadal white adipose was removed from lean, DIO and *ob/ob* mice ( $n=5$  per group) and stored at  $-80^\circ\text{C}$  in RNeasy Lysis Buffer (Qiagen, Austin, TX, USA). White adipose tissue total RNA was then extracted using RNeasy spin reagent (Qiagen) according to the manufacturer's instructions. Approximately 1  $\mu\text{g}$  of each RNA sample was subjected to DNase treatment immediately prior to reverse transcription into cDNA using the Superscript III First-Strand Synthesis System (Invitrogen, Carlsbad, CA, USA) as directed. The cDNA was then subjected to quantitative real-time PCR amplification using the Dynamo sybr green qPCR kit in an Opticon2 thermocycler (MJ Research, Waltham, MA, USA). Copy number of each target gene within any given cDNA sample was determined by extrapolating against a standard curve defined by serial 1:10 dilutions of pooled mouse adipose cDNA. Target gene copy number per given cDNA sample was then normalized to the copy number of a housekeeping gene hypoxanthine phosphoribosyl transferase (HPRT) for that sample. The PCR conditions were 40 cycles of  $94^\circ\text{C}/60^\circ\text{C}/72^\circ\text{C}$  at 15 s each. PCR primers were designed to span exon–intron boundaries to prevent genomic DNA amplification. The forward and reverse primers for each transcript were as follows: HIF-1 $\alpha$ : TCCATGTGACCATGAGGAAA and CTCCACGTTGCTGAC TTGA; HIF-2 $\alpha$ : AGTAGCCTCTGTGGCTCCAA and TCCAGG GCATGGTAGAACTC; HIF-1 $\beta$ : TCACGAAGGTCGTTTCATCTG and GATGTAGCCTGTGCAGTGGG; GLUT-1: ACTGGGCAA GTCCTTTGAGA and GTCTAAGCCAAACACCTGGGC HPRT: AGCAGTACAGCCCCAAA and TTTGGCTTTTCCAGTTTCA.

### Western blots

In a separate experiment, protein extracts (Active Motif, Carlsbad, CA, USA) were made from the entire perigonadal white adipose tissue depots obtained from lean wild-type C57BL/6J males, DIO wild-type C57BL/6J males and *ob/ob* C57BL/6J males ( $n=4$  per group). Fifty micrograms of protein per lane were electrophoresed under reducing conditions on a 10% bis-tris gel (NuPage, Invitrogen) and then transferred to a polyvinylidene difluoride membrane. After blocking, the membranes were hybridized to antibodies

for  $\beta$ -actin, HIF-1 $\alpha$  and GLUT-1 (sc-69879, sc-8711, sc-7903, Santa Cruz Biotechnology, Santa Cruz, CA, USA). Bands were exposed on the membrane using the WesternBreeze chromogenic kit (Invitrogen) and then quantified using NIH Image software.

#### *Hormone and cytokine assays*

After minimally fasting for 2 h to avoid any potentially acute fluctuations in glucose or leptin concentrations attributable to recent eating, six to eight mice per experimental group were weighed and then had their blood glucose measured by glucometer (Glucometer Elite, Elkhart, IN, USA) using approximately 5  $\mu$ l of tail tip blood. They were then killed by CO<sub>2</sub> asphyxiation. Their blood was then obtained by cardiac puncture, allowed to clot on ice for 3 h, and then centrifuged at 10000 g for 10 min. The sera were then transferred to clean vials for storage at  $-80^{\circ}$  C until the day of assay. Mouse serum insulin, leptin, MCP-1 (monocyte chemoattractant protein-1), adiponectin, resistin, tPAI-1 (tissue plasminogen activator-1), tumor necrosis factor- $\alpha$  and interleukin-6 were assayed by enzyme-linked immunosorbent assay (Linco Research Inc., St Charles, MO, USA). All inter- and intra-assay coefficients of variation were less than 10%.

#### *Real-time in vivo adipose tissue oxygen sensing*

In a separate experiment, at the age of approximately 28 weeks, four mice per group were weighed and then serially anesthetized by inhaling 2% isoflurane via nose cone with oxygen flow at 1 l/min. When completely anesthetized, a 5 mm incision was made in the right aspect of the lower abdomen of each mouse that was carried downward to the peritoneum. A 250  $\mu$ m diameter fiberoptic sensor for the simultaneous quantification of tissue  $pO_2$  and temperature (OxyLite, Oxford Optronix, Oxford, UK) was then inserted up to a depth of 3 mm in the perigonadal white adipose tissue of each mouse. Short pulses of LED light are transmitted along this fiberoptic sensor to excite a platinum-based fluorophore in the sensor tip. The degree to which this fluorescent light is quenched is directly proportional to the number of oxygen molecules within the surrounding tissue. The lifetime of fluorescence is inversely proportional to the concentration of dissolved oxygen, and is interpreted to provide an absolute value for  $pO_2$  in mm Hg.<sup>25</sup> This sensor detects and automatically compensates for the effects of temperature on  $pO_2$  readings by way of a small thermistor attached to its tip. A real-time reading of adipose  $pO_2$  and temperature was then made for approximately 60 s for each mouse.

#### *Immunohistochemistry*

The Hypoxyprobe kit (Chemicon, Temecula, CA, USA), which allows for the immunochemical detection of hypoxic

cellular conditions, was used according to the manufacturer's protocols. Hypoxyprobe consists of two principal components: a small molecule hypoxia marker, pimonidazole hydrochloride, that selectively binds to oxygen starved cells, and a monoclonal antibody, Hypoxyprobe-1-Mab1, that is used to detect pimonidazole adducts. Sixty minutes prior to killing, pimonidazole hydrochloride was injected intraperitoneally into lean, DIO and *ob/ob* male C57BL/6J mice at a concentration of 60  $\mu$ g/g body weight. Perigonadal white adipose tissue from each mouse was then dissected out and fixed overnight in 4% paraformaldehyde. Serial paraffin-embedded sections (7  $\mu$ m) were subsequently stained with Hypoxyprobe-1 monoclonal antibody (1:200), macrophage-specific F4/80 antibody (Chemicon) (1:100) or leukocyte-specific CD3 antibody (1:100). Secondary antibodies conjugated to horseradish peroxidase were utilized and counterstaining was performed according to previously described protocols.<sup>7</sup> For control purposes, one tissue slice was only stained with secondary antibody only.

#### *Flow cytometry*

At the age of approximately 24–28 weeks, six lean male wild-type C57BL/6J, six DIO male wild-type C57BL/6J and six male *ob/ob* C57BL/6J mice were killed by CO<sub>2</sub> asphyxiation and a sample of their perigonadal white adipose tissue was removed. Tissues were handled using sterile techniques and minced into fine (<10 mg) pieces. Minced samples were placed in HEPES-buffered DMEM (Invitrogen Corp.) supplemented with 10 mg/ml fatty acid-poor bovine serum albumin (Sigma-Aldrich, St Louis, MO, USA) and centrifuged at 1000 g for 10 min at room temperature to pellet erythrocytes and other blood cells. A lipopolysaccharide-depleted collagenase cocktail (Liberase Blendzyme 3; Roche Applied Science, Indianapolis, IN, USA) at a concentration of 0.03 mg/ml and 50 U/ml DNase I (Sigma-Aldrich) was added to the tissue suspension and the samples were incubated at 37 $^{\circ}$  C on an orbital shaker (215 Hz) for 45–60 min. Once digestion was complete, samples were passed through a sterile 250- $\mu$ m nylon mesh. The suspension was centrifuged at 1000 g for 10 min. The pelleted cells were the stromal vascular cells (SVCs), which were then resuspended in erythrocyte lysis buffer and incubated at room temperature for 5 min. The erythrocyte-depleted SVCs were centrifuged at 500 g for 5 min, and the pellet was resuspended in fluorescence-activated cell sorter (FACS) buffer (phosphate-buffered saline containing 5 mM EDTA and 0.2% (wt/vol) fatty acid-poor bovine serum albumin). In one experiment, the SVCs were stained only with antibodies recognizing the specific T-cell lineage markers CD4 and CD8 (BD Pharmingen, San Diego, CA, USA) in an attempt to assess the number of CD4<sup>+</sup>/CD8<sup>-</sup> or CD4<sup>-</sup>/CD8<sup>+</sup> cells relative to the entire SVC population.

In a different experiment, the SVCs were first stained for the universal T-cell lineage marker CD3, for which they were initially 'gated' in the FACS analysis in an attempt to assess

the proportion of each T-cell sub-type (CD3+/CD4+/CD8-, CD3+/CD4-/CD8+, CD3+/CD4-/CD8-) relative to one another. The LSR II Becton-Dickinson FACS was directed to perform flow cytometric analyses on 40 000 live cells per suspension using forward scatter, side scatter and 4,6-diamidino-2-phenylindole staining properties to identify live cells.

#### Statistics and definitions

Two-tailed student's *t*-tests were utilized to compare serum analytes between C57BL/6J lean and obese experimental groups. The lean mice were considered a control group to which each obese group was compared. All non-normally distributed data were analyzed with non-parametric testing.  $P < 0.05$  was considered statistically significant. All data were examined using Sigmapstat 2.0 software (Jandel Scientific, San Rafael, CA, USA).

## Results

#### Body composition/insulin sensitivity

The initial body weights of all mice at approximately 4 weeks of age were similar. By 28 weeks of age, the male C57BL/6J mice on the 35% fat diet were obese, weighing almost 100% more than their 4% fat fed controls ( $P < 0.001$ ). As expected, the leptin-deficient male *ob/ob* mice gained weight rapidly despite their low-fat diet and ultimately achieved the highest weights (Figure 1). As determined by DEXA scan, the DIO and *ob/ob* male mice possessed a nearly fourfold higher body fat percentage than the lean control group ( $P < 0.001$ ). The presence of obesity was associated with a significant diminution in the insulin sensitivity of male C57BL/6J mice as suggested by their significantly higher serum insulin levels (Figure 2a).

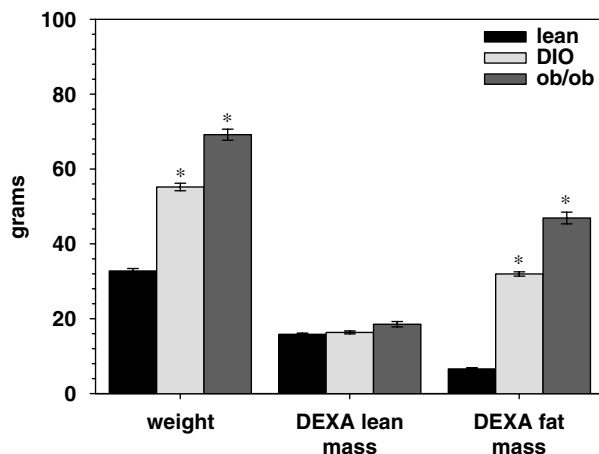


**Figure 1** Body composition and insulin sensitivity. Both high-fat diet and leptin deficiency induce obesity with significant increases in DEXA-determined body fat percentage ( $*P < 0.05$ ;  $N = 8$  per group; all data expressed as mean  $\pm$  s.e.m.). DEXA, dual energy X-ray absorptiometry.

#### Serum adipokine concentrations

Leptin levels were significantly increased in the DIO group compared to the lean group ( $P < 0.01$ ), while the *ob/ob* males demonstrated essentially no immunoreactive leptin as expected by the nature of their mutation (Figure 2c). Compared to the lean group, the serum levels of tPAI-1 and MCP-1, which are markers of inflammation previously demonstrated to correlate with both degree of obesity and extent of cardiovascular risk,<sup>26,27</sup> were noted to be significantly increased in both the DIO and *ob/ob* mice (Figures 2c and d). Resistin and adiponectin are adipokines whose serum levels have been shown to positively and negatively correlate, respectively, with the degree of insulin resistance.<sup>28,29</sup> While both the DIO and *ob/ob* mice manifested significant decreases in serum adiponectin compared to lean controls (Figure 2b), only the *ob/ob* mice manifested a significant increase in their serum resistin levels (Figure 2c), perhaps attributable to their greater duration and degree of obesity (Figure 2). In nearly all serum samples, the levels of tumor necrosis factor- $\alpha$  and interleukin-6 were below the detectable limit of their respective assays, and as such there are no data for these analytes.

#### White adipose tissue HIF and GLUT-1 expression

To investigate the presence of hypoxia within the visceral adipose tissue of obese mice, we performed real-time PCR on perigonadal adipose tissue cDNA using primers specific for GLUT-1 and HIF isoforms, two proteins notably upregulated by the presence of hypoxic conditions.<sup>30,31</sup> GLUT-1 is the predominant glucose transporter in macrophages, while adipocytes utilize GLUT-4. Compared to the lean group, the DIO and *ob/ob* male C57BL/6J mice were noted to manifest significantly increased adipose RNA expression of GLUT-1, HIF-1 $\alpha$  and HIF-2 $\alpha$  (Figure 3). The expression of HIF-1 $\beta$ , which is a constitutively expressed isoform, was not affected by obesity (Figure 3).

Western blots of perigonadal adipose tissue protein extracts revealed that HIF-1 $\alpha$  protein was increased in both DIO and *ob/ob* mice compared to the lean control group. GLUT-1 protein levels were increased in the adipose of *ob/ob* mice as compared to the lean mice (Figure 4).

#### White adipose tissue hypoxia and inflammation

Hypoxyprobe reagent contains pimonidazole, a compound with a well-described affinity for hypoxic cells.<sup>32-36</sup> The resulting hypoxic complexes are immunologically recognized by the Hypoxyprobe-1-mAB1 monoclonal antibody. White adipose tissue derived from lean male C57BL/6J mice was essentially devoid of Hypoxyprobe immunoreactivity (Figure 5a). There was sporadic cytoplasmic hypoxia staining in the interstitial stromal areas of the white adipose tissue from male DIO mice (Figure 5b), while more frequent and intense staining was noted in these areas in the white adipose derived from the *ob/ob* mice (Figure 5c).

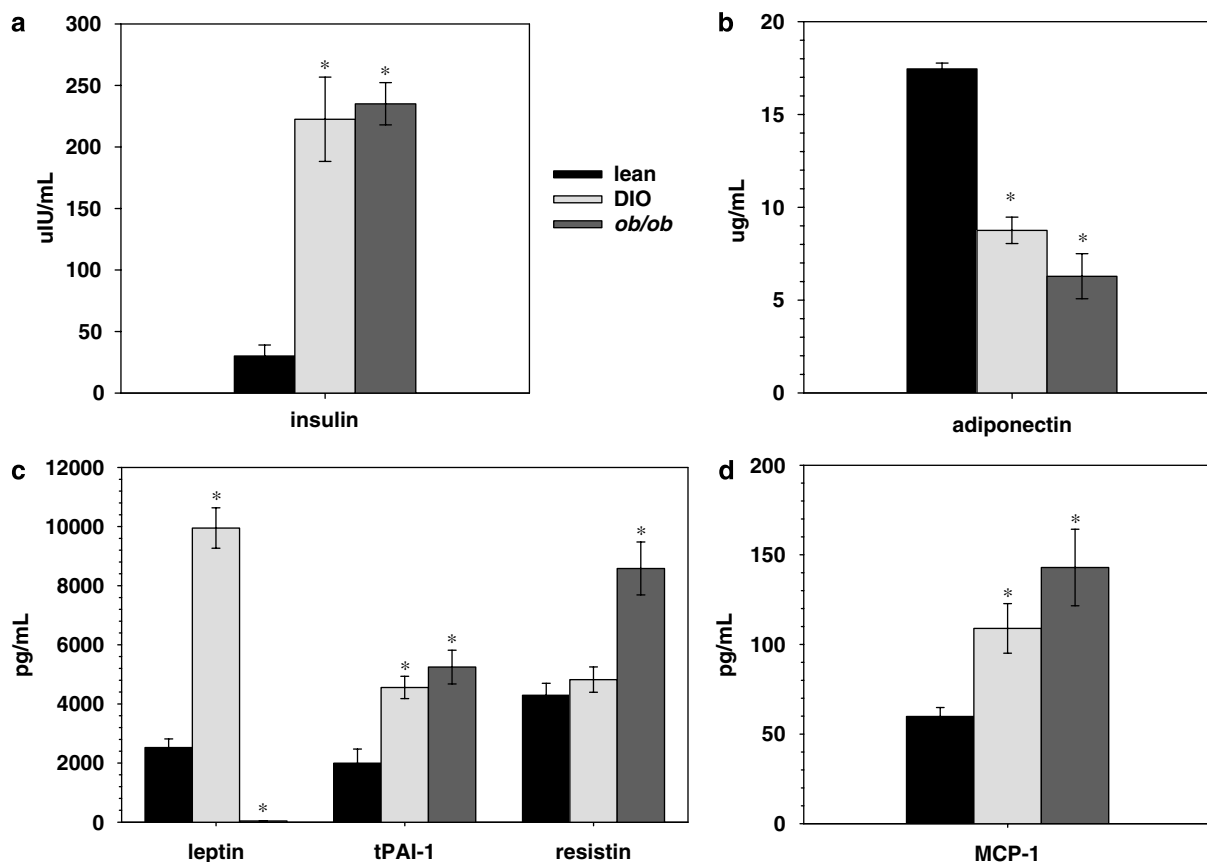


**Figure 2** Serum inflammatory markers are elevated in obese mice. Both DIO and *ob/ob* mice were noted to manifest significant pro-inflammatory/diabetogenic alterations in their serum levels of insulin, MCP-1, tPAI-1 and adiponectin as compared to the lean control group. The *ob/ob* mice, which achieve obesity earlier in life and to a more severe degree than DIO mice, also had a significant increase in their resistin levels (\* $P < 0.05$ ;  $N = 8$  per group; all data expressed as mean  $\pm$  s.e.m.). DIO, dietary-induced obese; MCP-1, monocyte chemoattractant protein-1; tPAI-1, tissue plasminogen activator-1.

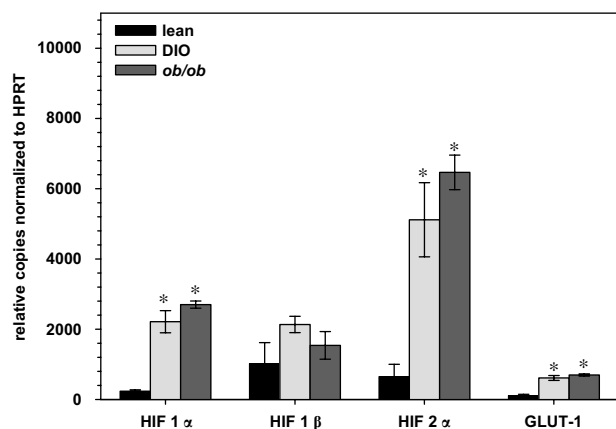


**Figure 3** Adipose HIF expression is higher in obese mice. As assessed by quantitative real-time PCR, the expression of HIF-1 $\alpha$ , HIF-2 $\alpha$  and GLUT-1, which are known to be upregulated under hypoxic conditions, was increased in both obese mouse groups compared to low fat fed lean wild-type mice. The expression of HIF-1 $\beta$ , a constitutively expressed protein, was not increased in obese mice (\* $P < 0.05$ ;  $N = 8$  per group; all data expressed as mean  $\pm$  s.e.m.). HIF, hypoxia-inducible factor.

#### In vivo assessment of adipose tissue $pO_2$

The OxyLite fluorometric oxygen sensor is a sensitive apparatus for the estimation of tissue oxygen content, and already has been extensively utilized by oncologists to assess tumor tissue hypoxia and perfusion for an estimation of sensitivity to systemic chemotherapy.<sup>37–39</sup> It is at its most sensitive at lower  $pO_2$  levels and, unlike polarographic electrodes, does not consume oxygen, which can lead to a false lower  $pO_2$  reading than is truly present.

The sensor revealed that the adipose tissue  $pO_2$  of lean C57BL/6J mice was consistently in the range of 35–40 mm Hg (Figure 6a), while that of the DIO and *ob/ob* mice was significantly lower and averaged only approximately 20 mm Hg (Figures 6b–d). Although every attempt was made to place the probes in identical fat pad locations among mice, there may have been some minute positional variations, accounting for some differences among adipose tissue temperatures. As temperature can slightly affect  $pO_2$  readings, the probe software is designed to compensate for any temperature differences encountered. No  $pO_2$  differences were noted among the kidneys between the three groups as assessed by this fluorometric sensor (not shown).

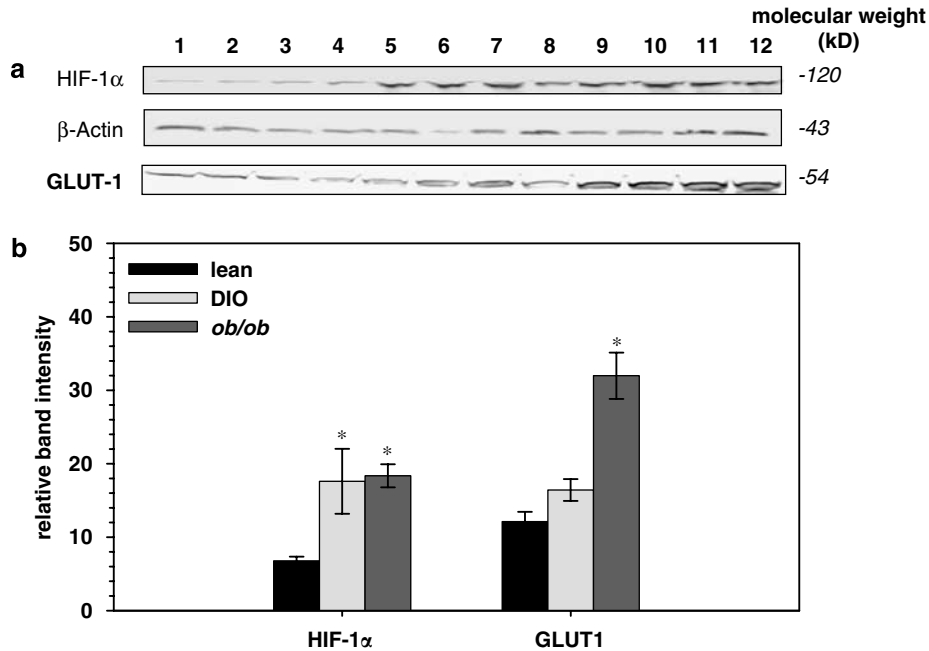


**Figure 4** Adipose HIF-1 $\alpha$  and GLUT-1 protein are increased in obese mice. Western blot of equal amounts of perigonadal adipose tissue protein extracts demonstrate that average HIF-1 $\alpha$  is increased in both DIO (lanes 5–8) and *ob/ob* (lanes 9–12) mice compared to lean controls (lanes 1–4), while GLUT-1 protein is increased in only the most obese group, the *ob/ob* mice. Approximate molecular mass is to the right of the blots (\* $P < 0.05$ ;  $N = 4$  per group; all data expressed as mean  $\pm$  s.e.m.). DIO, dietary-induced obese; HIF-1 $\alpha$ , hypoxia-inducible factor.

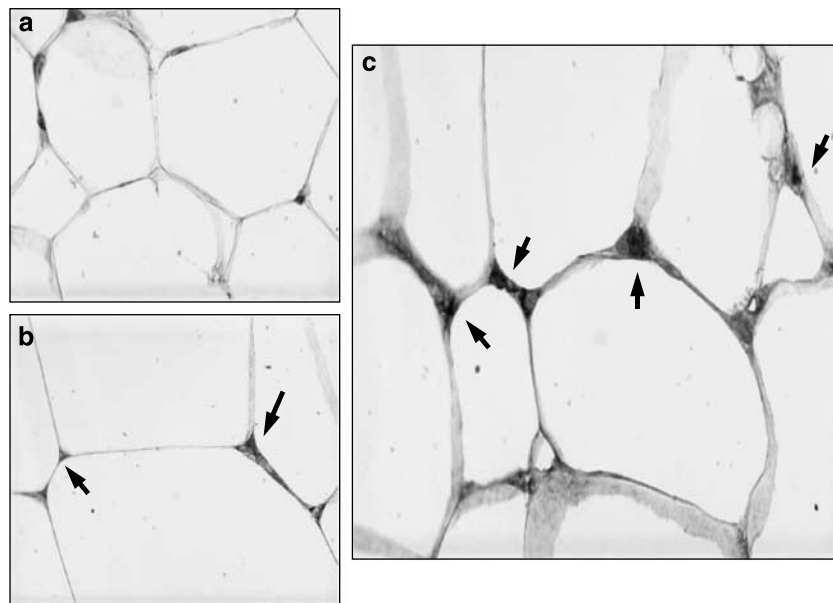


**Figure 5** Adipose of obese mice shows hypoxia immunoreactivity. Hypoxyprobe immunoreactivity (brown) is unseen in adipose tissue from 4% fat-fed lean mice (a), but is present in the cytoplasm of cells within the adipose stromal/vascular space of 35% fat-fed DIO mice (b) as well as *ob/ob* mice (c). DIO, dietary-induced obese.

#### Assessment of the cellular nature of adipose tissue hypoxia and inflammation

We hybridized adipose tissue with anti-F4/80 and anti-CD3 antibodies, which are specific for macrophages and T-cell

lymphocytes, respectively. We found F4/80+ macrophages encircling several individual adipocytes (Figure 7a) as well as occupying a predominantly peripheral location in several *ob/ob* inflammatory aggregates (Figures 7b–d). The areas

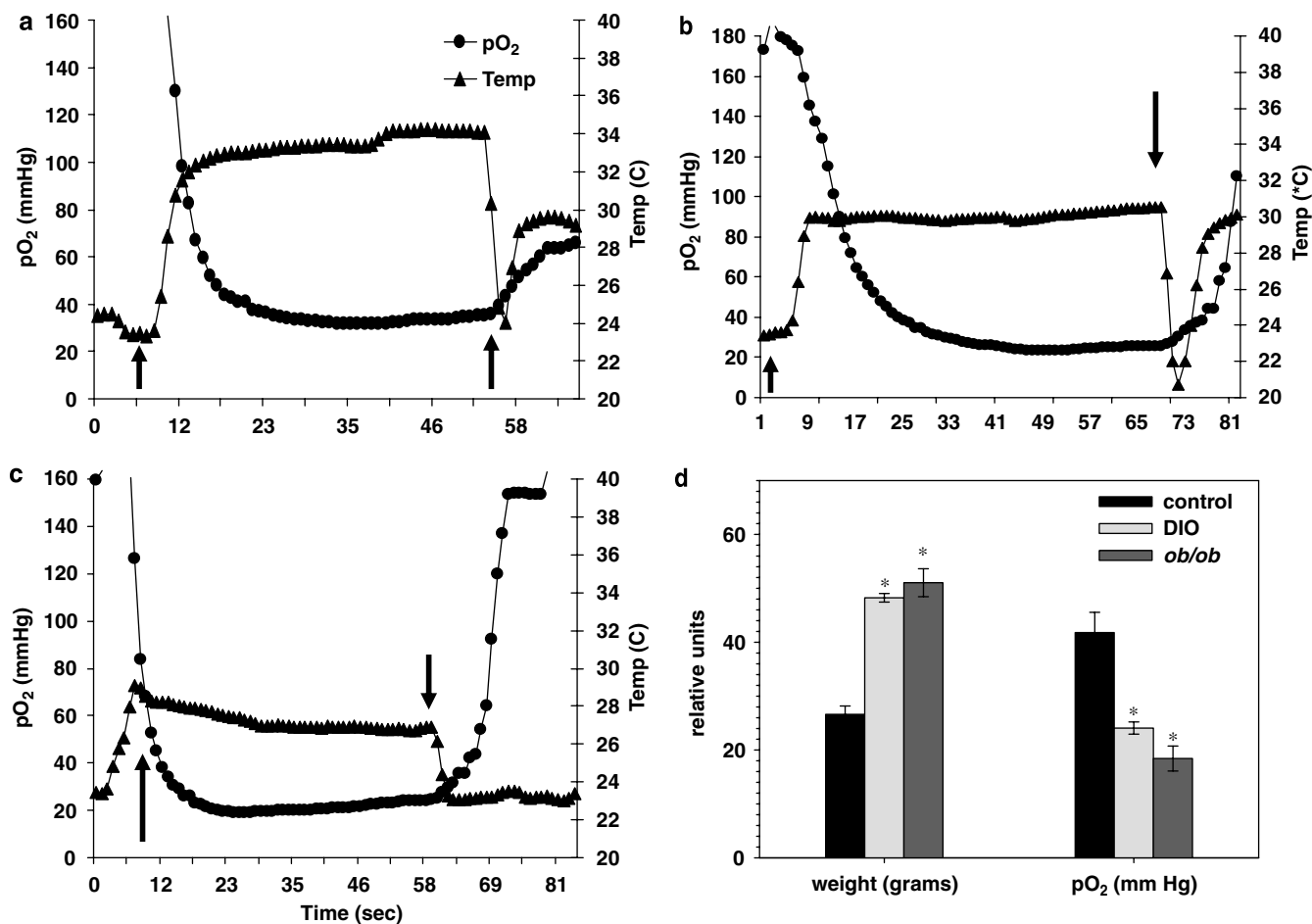


**Figure 6** *In vivo* adipose tissue oxygen status. Representative real-time read-outs of adipose tissue  $pO_2$  and temperature as determined by a fluorometric tissue oxygen sensor for lean (a), DIO (b) and *ob/ob* (c) male C57BL/6J mice are depicted. The area between the arrows indicates the time interval during which the probe was placed within the adipose tissue. After its insertion, the ambient  $pO_2$  and temperature readings declined and increased, respectively, to reflect the internal environment, and this reverses as the probe is removed. Both the DIO and *ob/ob* mice, which weighed approximately twice as much as the lean control mice, had real-time *in vivo* adipose tissue  $pO_2$  levels that were approximately half that of the lean control mice (d), suggesting that hypoxia is a feature common to obesity in male C57BL/6J mice ( $N=4$  per group; all data expressed as mean  $\pm$  s.e.m.). DIO, dietary-induced obese.

demonstrating immunoreactivity for hypoxia tended to colocalize with the F4/80+ macrophages in these inflammatory aggregates (Figures 8a and b). Interestingly, anti-CD3 immunoreactivity was present and quite intense among cells forming the central cluster within the inflammatory aggregates seen in the adipose tissue of the *ob/ob* mice (Figure 8c) and was also present encircling some individual adipocytes in both DIO and *ob/ob* mice (Figure 9a). Adipose tissue stained with anti-rabbit IgG secondary antibodies revealed no immunoreactivity (Figure 9b).

#### Flow cytometry

As false positive staining can result from the antibodies binding to Fc receptors on non-lymphoid cells, we used forward and side scatter to set a gate on small mononuclear cells and also preincubated cells with a 'nonsense' IgG.

We first performed FACS without pre-screening for the universal T-cell CD3 antigen in order to provide the clearest illustration of the absolute numbers of CD4+/CD8- and CD4-/CD8+ cells relative to the total number of viable adipose SVC cells counted (40 000). These cell populations are depicted in Figures 10a-c. We discovered that the stromal/vascular component of the perigonadal white adipose tissue from DIO and *ob/ob* mice (Figures 10b and c) contained approximately threefold more CD4-/CD8+ 'cytotoxic' T-cell lymphocytes than that of their lean wild-type cohorts (Figure 10a) with no significant difference between them with regard to the number of adipose CD4+/CD8- ('helper') T cells. There was a trend suggesting decreased CD4+/CD8- T cells in the *ob/ob* mice, which would be consistent with the fact that leptin contributes to their recruitment and activation.<sup>40</sup> The large population of CD4-/CD8- cells depicted on the dot-plots,

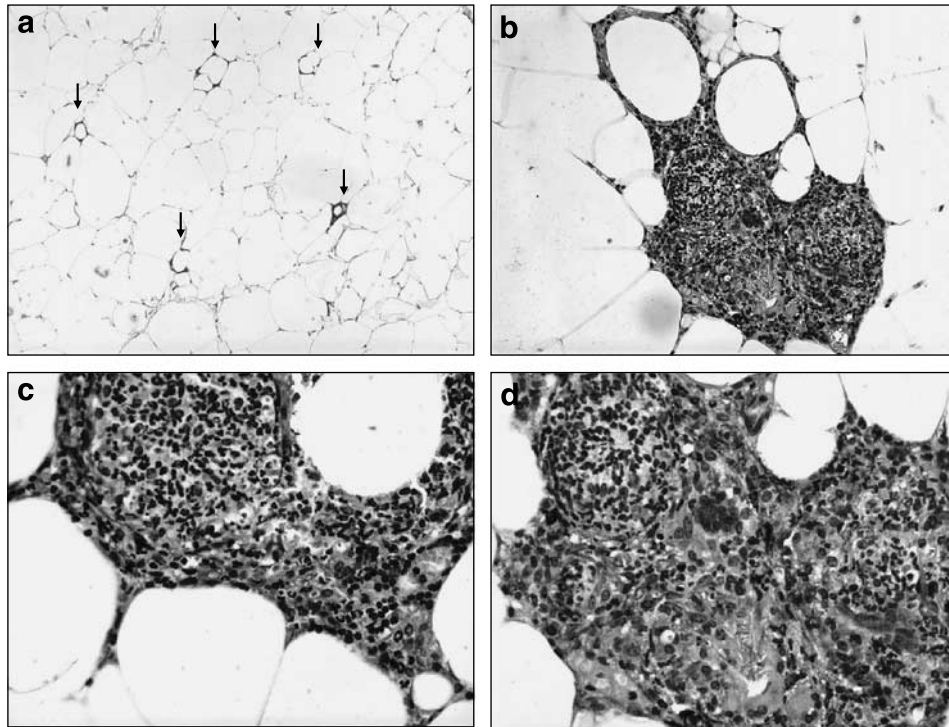


**Figure 7** Macrophages accumulate in *ob/ob* adipose tissue. Macrophage-specific F4/80 immunoreactivity in *ob/ob* mice is found surrounding individual adipocytes (see arrows in **a**) as well as predominantly peripherally in inflammatory aggregates (**b–d**).

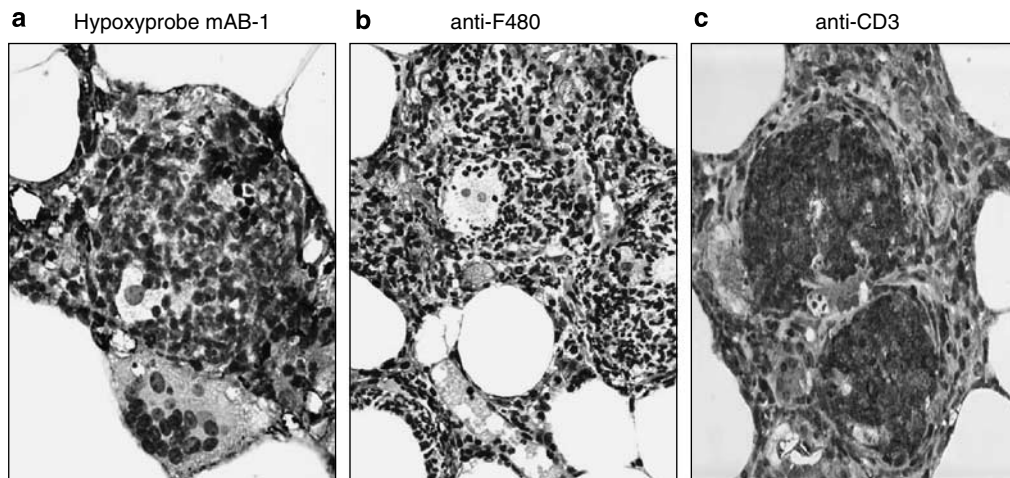


**Figure 8** Hypoxia and cellular inflammation in adipose tissue of *ob/ob* mice. Serial slices through the same inflammatory aggregate demonstrate a significant degree of overlapping between Hypoxyprobe and F4/80 immunoreactivity (**a**, **b**). There is also a striking influx of CD3+ T cells, which assume a central location within the aggregate in a configuration resembling a lymphoid follicle (**c**). Secondary antibody only treatments resulted in no immunoreactivity (not shown).

which did not vary between the experimental groups, consists mainly of the non-T cells in adipose tissue—mostly endothelial cells, macrophages, monocytes and preadipocytes.

When we first gated the SVC population for CD3+ status in the FACS analysis, we again noted a significant increase in the CD8+ T-cell subset (CD3+/CD4–/CD8+) among the

obese subgroups with no significant difference in the CD4+ (CD3+/CD4+/CD8–) or ‘double negative’ (CD3+/CD4–/CD8–) T-cell subsets (Figure 10d).

These findings are consistent with our immunohistochemical data and suggest that the nature of the adipose tissue inflammation in obese mice is a complex immunological phenomenon.

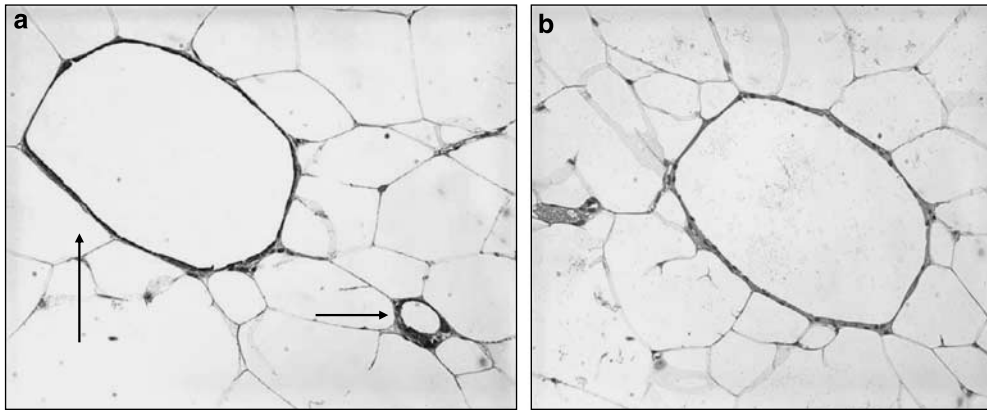


**Figure 9** CD3+ cells are present in *ob/ob* adipose tissue. CD3 immunoreactivity in *ob/ob* mice is also present sporadically encircling individual adipocytes (a). A serial slice of the adipocyte depicted in (a) stained only with secondary antibody reveals no immunoreactivity.

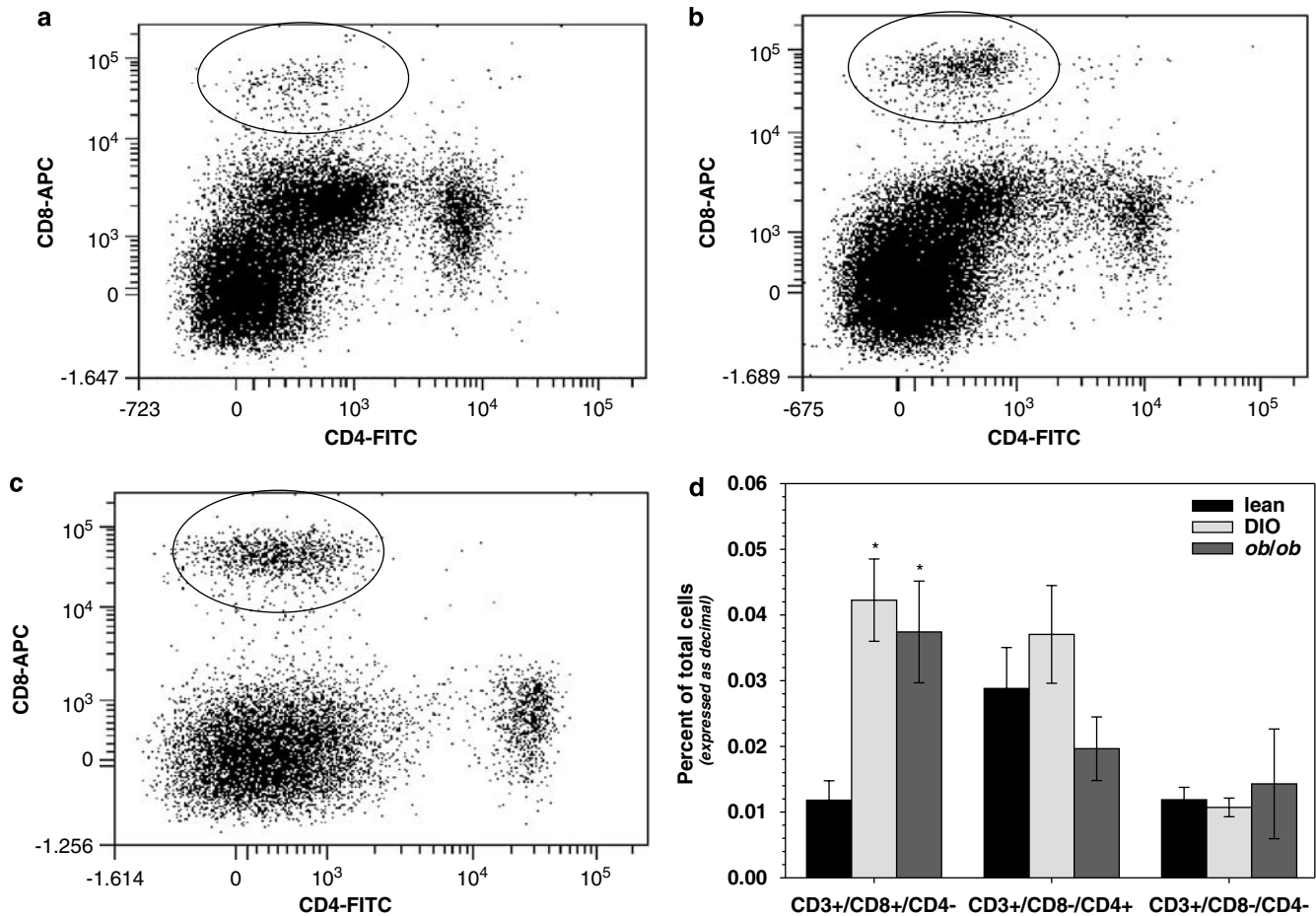


**Figure 10** Representative flow cytometric read-outs quantifying adipose tissue (CD4+ /CD8-) and (CD4-/CD8+) cells from lean (a), DIO (b) and *ob/ob* (c) male C57BL/6J mice. The FACS data are depicted without first gating for CD3+ cells in order to provide the clearest illustration of the numbers of CD4+ and CD8+ cells relative to the total number of viable cells recovered from adipose tissue. FACS reveals that the adipose of DIO and *ob/ob* male mice possess over threefold more cytotoxic CD8+ 'cytotoxic' T cells (seen within circles), with no significant differences in the number of CD4+ 'helper' T cells, compared to lean wild-type controls. The large population of CD4-/CD8- cells consists mainly of the non-T cells in adipose tissue—mostly endothelial cells, macrophages, monocytes and preadipocytes. In a separate experiment, we did initially stain or 'gate' for CD3-positive status. These populations are described by the bar graphs of (d). Again, only CD3+/CD4-/CD8+ cells were noted to be significantly increased in the obese mice. The number of double-negative T cells (CD3+/CD4-/CD8-) in this experiment was low, as would be expected for a site outside the thymus (\**P*<0.05; *N*=6 per group; all data expressed as mean ± s.e.m.).

## Discussion

Obesity is associated with macrophage infiltration of white adipose tissue. Pro-inflammatory alterations in the serum adipocytokine profile suggest that adipose inflammation 'spills over' into the systemic circulation of the obese, where it has been postulated to foster the development of obesity's numerous complications, especially insulin resistance.<sup>40</sup> Indeed, in this study, male C57BL/6J DIO and *ob/ob* mice, which possessed three- to fourfold higher body fat percentages as determined by DEXA imaging and manifested marked hyperinsulinemia compared to the low-fat fed wild-type control group.

Leptin, adiponectin and resistin are factors secreted primarily by adipocytes themselves rather than by their surrounding stromal cells and have major roles in the modulation of inflammation and insulin sensitivity. Leptin exerts mildly pro-inflammatory effects, activating macrophage phagocytosis and cytokine production,<sup>41</sup> and its increased expression in obesity may be partially attributable to the transactivation of its promoter by HIF-1.<sup>42</sup> Contrarily, adiponectin manifests anti-inflammatory activity, potentially by inhibiting macrophage production of tumor necrosis factor- $\alpha$  and interleukin-6.<sup>43</sup> Higher levels of adiponectin are found in leaner individuals and appear protective from the development of insulin-resistant diabetes. As would be expected, the obese mice in this study manifested significantly higher and lower serum leptin and adiponectin levels, respectively (Figure 2). Resistin has also been implicated in the pathogenesis of obesity-associated insulin resistance and type 2 diabetes mellitus in mouse models.<sup>40</sup> Even though the DIO and *ob/ob* mice we studied appeared to possess similar degrees of insulin resistance, serum resistin was significantly increased only in the *ob/ob* mice, a finding perhaps attributable to their much earlier onset of obesity.

We also noted that both the DIO and *ob/ob* mice manifested significant increases in their serum concentrations of the inflammatory markers tPAI-1 and MCP-1 (Figure 2). The increase in serum tPAI-1 levels in the obese mice is likely in response to the inflammatory environment of obesity.<sup>44,45</sup> MCP-1, a monocyte- and macrophage-specific chemoattractant,<sup>46</sup> is overexpressed in the white adipose tissue of both obese mice and humans, and the elevated serum levels that this generates are normalized by weight loss.<sup>47</sup>

When the vascular supply feeding adipose tissue was made profoundly insufficient through inhibition of angiogenesis, the ability to develop obesity was significantly impaired.<sup>48</sup> This suggests that the vascularity of adipose tissue plays a large role in its ability to expand. Given the fact that our high-fat fed and *ob/ob* mice do indeed become quite obese, it is unlikely that their adipose vasculature is profoundly deficient, but it is reasonable to hypothesize that the vasculature support of rapidly enlarging white adipose tissue may prove marginal, rendering it susceptible to intermittent

local hypoxia in times of rapid lipid accumulation. This in turn may foster premature adipocyte death and adipose tissue inflammation. Consistent with this is a recent ultrastructural study, which has demonstrated that obesity in both mice and humans is associated with up to a thirty-fold increase in adipocyte death, a finding that positively correlated with both adipocyte size and adipose tumor necrosis factor- $\alpha$  gene expression.<sup>49</sup> The plausibility of this hypothesis becomes evident when one considers the fact that, during the development of obesity, adipocytes can hypertrophy to diameters nearly twice the diffusion limit of oxygen into cells.<sup>50,51</sup>

We first tested this premise indirectly by quantifying the expression of adipose genes known to be upregulated by hypoxic conditions, namely HIF-1 $\alpha$ , HIF-2 $\alpha$  and GLUT-1.<sup>52-55</sup> Consistent with our hypothesis, we noted their expression to be increased by quantitative real-time PCR in the adipose tissue of both DIO and *ob/ob* mice as compared to lean controls. As HIF-1 $\beta$  levels are constitutively expressed and not influenced by hypoxia, one would expect to find equivalent levels in both obese and lean mice, as were our findings here. HIF-1 $\alpha$  protein levels were also increased in both DIO and *ob/ob* mice, consistent with the PCR data (Figure 4).

Under hypoxic conditions, HIF-1 $\alpha$  and HIF-2 $\alpha$  migrate to the cell's nucleus where they bind to the  $\beta$ -subunit. These functional HIF dimers then bind to hypoxia-responsive elements in the promoter and enhancer regions of target genes to stimulate the expression of angiogenic and inflammatory mediators. Both adipocytes and macrophages increase their expression of potent angiogenic hormones in response to hypoxia, primarily via induction of HIF-1.<sup>56,57</sup> Interestingly, recent reports suggest that HIF-1 may also modulate macrophage recruitment into inflammatory lesions.<sup>56</sup>

Although GLUT-1 mRNA expression was increased in the adipose of both DIO and *ob/ob* mice, we noted that GLUT-1 protein was only increased in the *ob/ob* mice, which were the most obese group. GLUT-1 is a plasma membrane glucose transporter whose primary role is to mediate basal glucose uptake independent of insulin concentration. GLUT-1 has been shown to be upregulated by hypoxia in primary human monocyte-derived macrophages as well as in murine peritoneal macrophages,<sup>56</sup> an event that likely promotes survival by facilitating glycolysis during periods of oxygen deprivation. Given this, as well as the fact that the primary glucose transporter of the adipocyte itself is GLUT-4, the increased expression of adipose GLUT-1 we observed in obese mice is likely attributable to its increased transcription in macrophages, which have accumulated within the stromal/vascular compartment of adipose tissue rather than the adipocytes themselves.

Using a pimonidazole-based antibody system, we determined that hypoxia is present in the adipose tissue of obese male C57BL/6J mice. Adipose tissue from lean wild-type male mice bore almost no evidence of pimonidazole

immunoreactivity, while their DIO cohorts manifested fairly robust stromal-vascular cell cytoplasmic staining. The most intense and frequent cytoplasmic staining, however, was noted in the white adipose tissue of *ob/ob* mice (Figure 5c). Consistent with the pimonidazole data, both DIO and *ob/ob* mice manifested significantly lower *in vivo* adipose  $pO_2$  levels compared to the lean control group as discerned by a sensitive fluorometric oxygen sensor (Figure 6).

Using immunohistochemistry, we noted increased numbers of CD3+ T cells as well as F4/80+ macrophages in white adipose tissue derived from obese *ob/ob* mice as compared to lean mice. Both cell types were intermittently found surrounding individual adipocytes. In the *ob/ob* mice, large inflammatory aggregates were also seen, in which CD3+ T cells were noted to form central circular clusters around which F4/80+ macrophages gathered. It will be very interesting to determine whether these central CD3+ cells are of the CD4 or CD8 subset; if these cells were CD4+, it would suggest these clusters to be 'ectopic germinal centers'. Unfortunately, the current gamut of CD3 and CD4 antibodies is optimally suited for FACS analysis, not immunohistochemistry, and this was our impetus to perform FACS on the adipose tissue SVCs rather than immunohistochemistry to further characterize the CD3+ cell population.

The fact that the areas of hypoxia overlapped to a large extent with the presence of macrophage-specific F4/80 immunoreactivity (Figure 8) suggests that macrophages may be drawn to areas of relative hypoxia in white adipose tissue, and in such a milieu, become relatively hypoxic themselves. This would be consistent with recent evidence demonstrating that macrophages accumulate in extraordinarily high numbers in the hypoxic areas of various carcinomas, and are in fact at their most plentiful in tumors manifesting the highest degree of hypoxia.<sup>58</sup> As macrophages are cells that phagocytize necrotic debris, it is not surprising that they have been found encircling dead adipocytes in obese mice and humans.<sup>49</sup>

FACS analysis revealed that cells from the CD8+, but not CD4+, T-cell lineage are significantly increased in the adipose from obese mice (Figures 10a-c). The significantly increased presence of T cells from the CD8+, but not CD4+, subset in the adipose of obese male mice suggests that adipose tissue macrophages may serve to attract and/or enhance the function of CD8+ cells. This raises the intriguing possibility that macrophage-facilitated CD8+ T-cell destruction of adipocytes may be occurring, a phenomenon, which has been implicated in certain autoimmune diseases such as type 1 diabetes.<sup>59</sup> In fact, MCP-1, the expression of which in obese rodents and humans is increased in proportion to adiposity, has recently been shown to be a very potent activator of CD8+ cytotoxic activity.<sup>59</sup>

In conclusion, we have shown evidence that obesity and systemic inflammation are associated with hypoxic conditions in the perigonadal white adipose tissue of male C57BL/6J mice. Consistent with this, we have documented

increased adipose tissue expression of GLUT-1 and HIF-1 $\alpha$ . Moreover, utilizing a highly sensitive fluorometric tissue oxygen sensor, we have determined that the  $pO_2$  in the perigonadal adipose tissue of both dietary and genetically induced obese mice is significantly lower than that of lean controls. Hypoxia in adipose tissue was noted to primarily colocalize with the presence of F4/80+ macrophages, suggesting that in a manner similar to that, which occurs in tumor tissue, macrophages migrate into hypoxic regions of adipose tissue where they alter their expression profile in a manner that fosters inflammatory changes. We have also documented the novel finding that CD8+ T cells, in addition to macrophages, accumulate in the white adipose tissue of dietary and genetically induced obese C57BL/6J mice. This finding raises the possibility that T-cell-mediated cytotoxicity may be contributing to this inflammatory process, and the function of macrophages may be to attract or enhance the function of activated CD8+ cells.

Although leukocyte-induced inflammation may precipitate adipocyte cell death and hypoxia, we hypothesize that adipocyte hypoxic cell death occurs initially, followed by leukocyte recruitment and then an enhanced release of inflammatory adipocytokines. To delineate the actual sequence of events, larger studies examining serum and adipose markers of hypoxia and inflammation at several time points during the gradual development of an obese state will be required.

## Acknowledgements

This work was supported by a Women's Reproductive Health Research Scholarship, NIH 5 K12 HD001275-04 (DVT).

## References

- 1 Mendez MA, Monteiro CA, Popkin BM. Overweight exceeds underweight among women in most developing countries. *Am J Clin Nutr* 2005; **81**: 714-721.
- 2 Rigby NJ, Kumanyika S, James WP. Confronting the epidemic: the need for global solutions. *J Public Health Policy* 2004; **25**: 418-434.
- 3 Pi-Sunyer FX. The obesity epidemic: pathophysiology and consequences of obesity. *Obes Res* 2002; **10** (Suppl 2): 97S-104S.
- 4 Mokdad AH, Bowman BA, Ford ES, Vinicor F, Marks JS, Koplan JP. The continuing epidemics of obesity and diabetes in the United States. *JAMA* 2001; **286**: 1195-1200.
- 5 Mokdad AH, Ford ES, Bowman BA, Dietz WH, Vinicor F, Bales VS et al. Prevalence of obesity, diabetes, and obesity-related health risk factors, 2001. *JAMA* 2003; **289**: 76-79.
- 6 Speiser PW, Rudolf MC, Anhalt H, Camacho-Hubner C, Chiarelli F, Eliakim A et al. Childhood obesity. *J Clin Endocrinol Metab* 2005; **90**: 1871-1887.
- 7 Weisberg SP, McCann D, Desai M, Rosenbaum M, Leibel RL, Ferrante Jr AW. Obesity is associated with macrophage accumulation in adipose tissue. *J Clin Invest* 2003; **112**: 1796-1808.
- 8 Berg AH, Scherer PE. Adipose tissue, inflammation, and cardiovascular disease. *Circ Res* 2005; **96**: 939-949.
- 9 Browning JD, Horton JD. Molecular mediators of hepatic steatosis and liver injury. *J Clin Invest* 2004; **114**: 147-152.

- 10 Wellen KE, Hotamisligil GS. Inflammation, stress, and diabetes. *J Clin Invest* 2005; **115**: 1111–1119.
- 11 Pickup JC. Inflammation and activated innate immunity in the pathogenesis of type 2 diabetes. *Diabetes Care* 2004; **27**: 813–823.
- 12 Hotamisligil GS, Shargill NS, Spiegelman BM. Adipose expression of tumor necrosis factor- $\alpha$ : direct role in obesity-linked insulin resistance. *Science* 1993; **259**: 87–91.
- 13 Bastard JP, Jardel C, Delattre J, Hainque B, Bruckert E, Oberlin F. Evidence for a link between adipose tissue interleukin-6 content and serum C-reactive protein concentrations in obese subjects. *Circulation* 1999; **99**: 2221–2222.
- 14 Fried SK, Bunkin DA, Greenberg AS. Omental and subcutaneous adipose tissues of obese subjects release interleukin-6: depot difference and regulation by glucocorticoid. *J Clin Endocrinol Metab* 1998; **83**: 847–850.
- 15 Lin HZ, Yang SQ, Chuckaree C, Kuhajda F, Ronnet G, Diehl AM. Metformin reverses fatty liver disease in obese, leptin-deficient mice. *Nat Med* 2000; **6**: 998–1003.
- 16 Cai D, Yuan M, Frantz DE, Melendez PA, Hansen L, Lee J *et al*. Local and systemic insulin resistance resulting from hepatic activation of IKK- $\beta$  and NF- $\kappa$ B. *Nat Med* 2005; **11**: 183–190.
- 17 Brodmerkel CM, Huber R, Covington M, Diamond S, Hall L, Collins R *et al*. Discovery and pharmacological characterization of a novel rodent-active CCR2 antagonist, INCB3344. *J Immunol* 2005; **175**: 5370–5378.
- 18 Skurk T, Hauner H. Obesity and impaired fibrinolysis: role of adipose production of plasminogen activator inhibitor-1. *Int J Obes Relat Metab Disord* 2004; **28**: 1357–1364.
- 19 Arkan MC, Hevener AL, Greten FR, Maeda S, Li ZW, Long JM *et al*. IKK- $\beta$  links inflammation to obesity-induced insulin resistance. *Nat Med* 2005; **11**: 191–198.
- 20 Hirosumi J, Tuncman G, Chang L, Gorgun CZ, Uysal KT, Maeda K *et al*. A central role for JNK in obesity and insulin resistance. *Nature* 2002; **420**: 333–336.
- 21 Yuan M, Konstantopoulos N, Lee J, Hansen L, Li ZW, Karin M *et al*. Reversal of obesity- and diet-induced insulin resistance with salicylates or targeted disruption of Ikk $\beta$ . *Science* 2001; **293**: 1673–1677.
- 22 Curat CA, Miranville A, Sengenès C, Diehl M, Tonus C, Busse R *et al*. From blood monocytes to adipose tissue-resident macrophages: induction of diapedesis by human mature adipocytes. *Diabetes* 2004; **53**: 1285–1292.
- 23 Xu H, Barnes GT, Yang Q, Tan G, Yang D, Chou CJ *et al*. Chronic inflammation in fat plays a crucial role in the development of obesity-related insulin resistance. *J Clin Invest* 2003; **112**: 1821–1830.
- 24 Semenza GL. HIF-1: mediator of physiological and pathophysiological responses to hypoxia. *J Appl Physiol* 2000; **88**: 1474–1480.
- 25 Griffiths JR, Robinson SP. The OxyLite: a fibre-optic oxygen sensor. *Br J Radiol* 1999; **72**: 627–630.
- 26 Alessi MC, Juhan-Vague I. Contribution of PAI-1 in cardiovascular pathology. *Arch Mal Coeur Vaiss* 2004; **97**: 673–678.
- 27 Hoogeveen RC, Morrison A, Boerwinkle E, Miles JS, Rhodes CE, Sharrett AR *et al*. Plasma MCP-1 level and risk for peripheral arterial disease and incident coronary heart disease: Atherosclerosis Risk in Communities study. *Atherosclerosis* 2005; **183**: 301–307.
- 28 Silha JV, Krsek M, Skrha JV, Sucharda P, Nyomba BL, Murphy LJ. Plasma resistin, adiponectin and leptin levels in lean and obese subjects: correlations with insulin resistance. *Eur J Endocrinol* 2003; **149**: 331–335.
- 29 Garg A. Adipose tissue dysfunction in obesity and lipodystrophy. *Clin Cornerstone* 2006; **8** (Suppl 4): S7–S13.
- 30 Gleadle JM, Ratcliffe PJ. Induction of hypoxia-inducible factor-1, erythropoietin, vascular endothelial growth factor, and glucose transporter-1 by hypoxia: evidence against a regulatory role for Src kinase. *Blood* 1997; **89**: 503–509.
- 31 Zhou JT, Cai ZM, Li NC, Na YQ. Expression of hypoxia inducible factor-1 $\alpha$  and glucose transporter protein 1 in renal and bladder cancers and the clinical significance thereof. *Zhonghua Yi Xue Za Zhi* 2006; **86**: 1970–1974.
- 32 Yaromina A, Zips D, Thames HD, Eicheler W, Krause M, Rosner A *et al*. Pimonidazole labelling and response to fractionated irradiation of five human squamous cell carcinoma (hSCC) lines in nude mice: The need for a multivariate approach in biomarker studies. *Radiother Oncol* 2006; **81**: 122–129.
- 33 Tanaka T, Kato H, Kojima I, Ohse T, Son D, Tawakami T *et al*. Hypoxia and expression of hypoxia-inducible factor in the aging kidney. *J Gerontol A Biol Sci Med Sci* 2006; **61**: 795–805.
- 34 Troost EG, Laverman P, Kaanders JH, Philippens M, Lok J, Oyen WJ *et al*. Imaging hypoxia after oxygenation-modification: comparing [18F]FMISO autoradiography with pimonidazole immunohistochemistry in human xenograft tumors. *Radiother Oncol* 2006; **80**: 157–164.
- 35 Nordmark M, Lancaster J, Aquino-Parsons C, Chou SC, GebSKI V, West C *et al*. The prognostic value of pimonidazole and tumour pO<sub>2</sub> in human cervix carcinomas after radiation therapy: a prospective international multi-center study. *Radiother Oncol* 2006; **80**: 123–131.
- 36 Jankovic B, Aquino-Parsons C, Raleigh JA, Stanbridge EJ, Durand RE, Banath JP *et al*. Comparison between pimonidazole binding, oxygen electrode measurements, and expression of endogenous hypoxia markers in cancer of the uterine cervix. *Cytometry B Clin Cytom* 2006; **70**: 45–55.
- 37 Urano M, Chen Y, Humm J, Koutcher JA, Zanzonico P, Ling C. Measurements of tumor tissue oxygen tension using a time-resolved luminescence-based optical oxyLite probe: comparison with a paired survival assay. *Radiat Res* 2002; **158**: 167–173.
- 38 Braun RD, Lanzen JL, Snyder SA, Dewhirst MW. Comparison of tumor and normal tissue oxygen tension measurements using OxyLite or microelectrodes in rodents. *Am J Physiol Heart Circ Physiol* 2001; **280**: H2533–H2544.
- 39 Wen B, Urano M, O'Donoghue JA, Ling CC. Measurements of partial oxygen pressure pO<sub>2</sub> using the OxyLite system in R3327-AT tumors under isoflurane anesthesia. *Radiat Res* 2006; **166**: 512–518.
- 40 Tilg H, Moschen AR. Adipocytokines: mediators linking adipose tissue, inflammation and immunity. *Nat Rev Immunol* 2006; **6**: 772–783.
- 41 Loffreda S, Yang SQ, Lin HZ, Karp CL, Brengman ML, Wang DJ *et al*. Leptin regulates proinflammatory immune responses. *FASEB J* 1998; **12**: 57–65.
- 42 Grosfeld A, Andre J, Hauguel-De Mouzon S, Berra E, Pousyssegur J, Guerre-Millo M. Hypoxia-inducible factor 1 transactivates the human leptin gene promoter. *J Biol Chem* 2002; **277**: 42953–42957.
- 43 Tsatsanis C, Zacharioudaki V, Androulidaki A, Dermitzaki E, Charalampopoulos I, Minas V *et al*. Adiponectin induces TNF- $\alpha$  and IL-6 in macrophages and promotes tolerance to itself and other pro-inflammatory stimuli. *Biochem Biophys Res Commun* 2005; **335**: 1254–1263.
- 44 Mertens I, Verrijken A, Michiels JJ, Van der Planken M, Ruige JB, Van Gaal LF. Among inflammation and coagulation markers, PAI-1 is a true component of the metabolic syndrome. *Int J Obes (London)* 2006; **30**: 1308–1314.
- 45 Tortoriello DV, McMinn JE, Chua SC. Increased expression of hypothalamic leptin receptor and adiponectin accompany resistance to dietary-induced obesity and infertility in female C57BL/6j mice. *Int J Obes (London)* 2006; **31**: 395–402.
- 46 Weisberg SP, Hunter D, Huber R, Lemieux J, Slaymaker S, Vaddi K *et al*. CCR2 modulates inflammatory and metabolic effects of high-fat feeding. *J Clin Invest* 2005; **116**: 115–124.
- 47 Canello R, Henegar C, Viguier N, Taleb S, Poitou C, Rouault C *et al*. Reduction of macrophage infiltration and chemoattractant gene expression changes in white adipose tissue of morbidly obese subjects after surgery-induced weight loss. *Diabetes* 2005; **54**: 2277–2286.

- 48 Kim YM, An JJ, Jin YJ, Rhee Y, Cha BS, Lee HC *et al*. Assessment of the anti-obesity effects of the TNP-470 analog, CKD-732. *J Mol Endocrinol* 2007; **38**: 455–465.
- 49 Cinti S, Mitchell G, Barbatelli G, Murano I, Ceresi E, Faloia E *et al*. Adipocyte death defines macrophage localization and function in adipose tissue of obese mice and humans. *J Lipid Res* 2005; **46**: 2347–2355.
- 50 Helmlinger G, Yuan F, Dellian M, Jain RK. Interstitial pH and pO<sub>2</sub> gradients in solid tumors *in vivo*: high-resolution measurements reveal a lack of correlation. *Nat Med* 1997; **3**: 177–182.
- 51 Brook CG, Lloyd JK, Wolf OH. Relation between age of onset of obesity and size and number of adipose cells. *BMJ* 1972; **2**: 25–27.
- 52 Bianciardi P, Fantacci M, Caretti A, Ronchi R, Milano G, Morel S *et al*. Chronic *in vivo* hypoxia in various organs: hypoxia-inducible factor-1alpha and apoptosis. *Biochem Biophys Res Commun* 2006; **342**: 875–880.
- 53 Haase VH. Hypoxia-inducible factors in the kidney. *Am J Physiol Renal Physiol* 2006; **291**: F271–F281.
- 54 Papandreou I, Cairns RA, Fontana L, Lim AL, Denko NC. HIF-1 mediates adaptation to hypoxia by actively downregulating mitochondrial oxygen consumption. *Cell Metab* 2006; **3**: 187–197.
- 55 Burke B, Giannoudis A, Corke KP, Gill D, Wells M, Ziegler-Heitbrock L *et al*. Hypoxia-induced gene expression in human macrophages: implications for ischemic tissues and hypoxia-regulated gene therapy. *Am J Pathol* 2003; **163**: 1233–1243.
- 56 Cramer T, Yamanishi Y, Clausen BE, Forster I, Pawlinski R, Mackman N *et al*. HIF-1alpha is essential for myeloid cell-mediated inflammation. *Cell* 2003; **112**: 645–657.
- 57 Lewis JS, Landers RJ, Underwood JC, Harris AL, Lewis CE. Expression of vascular endothelial growth factor by macrophages is up-regulated in poorly vascularized areas of breast carcinomas. *J Pathol* 2000; **192**: 150–158.
- 58 Leek RD, Landers RJ, Harris AL, Lewis CE. Necrosis correlates with high vascular density and focal macrophage infiltration in invasive carcinoma of the breast. *Br J Cancer* 1999; **79**: 991–995.
- 59 Jarpe AJ, Hickman MR, Anderson JT, Winter WE, Peck AB. Flow cytometric enumeration of mononuclear cell populations infiltrating the islets of Langerhans in prediabetic NOD mice: development of a model of autoimmune insulinitis for type I diabetes. *Reg Immunol* 1990; **3**: 305–317.